

Exclusive Dilepton Production

Jakub Wagner

Theoretical Physics Department
National Centre for Nuclear Research, Warsaw

1st International Workshop on a 2nd Detector for the EIC, 19 May 2023

In collaboration with:

B. Pire, L. Szymanowski, P. Sznajder, H. Moutarde, O. Grocholski (**TCS**)

K. Deja, B. Pire, P. Sznajder, V. Martínez-Fernández (**DDVCS**) - arXiv:2303.13668 PRD??

In addition to spacelike DVCS ...

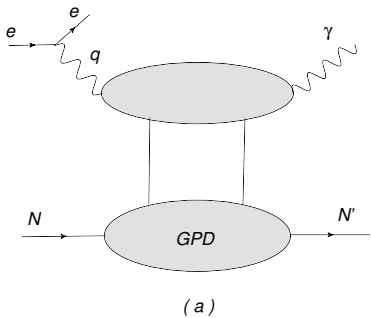


Figure: Deeply Virtual Compton Scattering (DVCS) : $lN \rightarrow l'N'\gamma$

we MUST also study timelike DVCS

Berger, Diehl, Pire, 2002

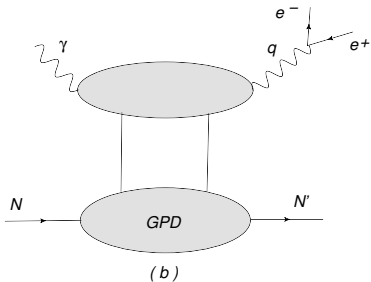


Figure: Timelike Compton Scattering (TCS): $\gamma N \rightarrow l^+ l^- N'$

Why TCS:

- ▶ same proven factorization properties as DVCS
- ▶ universality of the GPDs
- ▶ another source for GPDs (special sensitivity on real part of GPD H),
- ▶ the same final state as in J/ψ , but cleaner theoretical description!

First Measurement of Timelike Compton Scattering

P. Chatagnon,^{20,*} S. Niccolai,²⁰ S. Stepanyan,³⁶ M. J. Amaryan,²⁹ G. Angelini,¹² W. R. Armstrong,¹ H. Atac,³⁵ C. Ayerbe Gayoso,^{44,†} N. A. Baltzell,³⁶ L. Barion,¹³ M. Bashkanov,⁴² M. Battaglieri,^{36,15} I. Bedlinskiy,²⁵ F. Benmokhtar,⁷ A. Bianconi,^{39,19} L. Biondo,^{15,18,40} A. S. Biselli,⁸ M. Bondi,¹⁵ F. Bossù,³ S. Boiarinov,³⁶ W. J. Briscoe,¹² W. K. Brooks,^{37,36} D. Bulumulla,²⁹ V. D. Burkert,³⁶ D. S. Carman,³⁶ J. C. Carvajal,¹⁰ M. Caudron,²⁰ A. Celentano,¹⁵ T. Chetry,^{24,28} G. Ciullo,^{13,9} L. Clark,⁴¹ P. L. Cole,²² M. Contalbrigo,¹³ G. Costantini,^{39,19} V. Crede,¹¹ A. D'Angelo,^{16,32} N. Dashyan,⁴⁵ M. Defurne,³ R. De Vita,¹⁵ A. Deur,³⁶ S. Diehl,^{30,5} C. Djalali,²⁸ R. Dupré,²⁰ H. Egiyan,³⁶ M. Ehrhart,^{20,‡} A. El Alaoui,³⁷ L. El Fassi,²⁴ L. Elouadhrhi,³⁶ S. Fegan,⁴² R. Fersch,⁴ A. Filippi,¹⁷ G. Gavalian,³⁶ Y. Ghandilyan,⁴⁵ G. P. Gilfoyle,³¹ F. X. Girod,³⁶ D. I. Glazier,⁴¹ A. A. Golubenko,³³ R. W. Gothe,³⁴ Y. Gorla,³⁶ K. A. Griffioen,⁴⁴ M. Guidal,²⁰ L. Guo,¹⁰ H. Hakobyan,^{37,45} M. Hattaway,²⁹ T. B. Hayward,^{5,44} D. Heddle,^{4,36} A. Hobart,²⁰ M. Holtrop,²⁶ C. E. Hyde,²⁹ Y. Ilieva,³⁴ D. G. Ireland,⁴¹ E. L. Isupov,³³ H. S. Jo,²¹ K. Joo,⁵ M. L. Kabir,²⁴ D. Keller,⁴³ G. Khachatryan,⁴⁵ A. Khanal,¹⁰ A. Kim,⁵ W. Kim,²¹ A. Kripko,³⁰ V. Kubarovsky,³⁶ S. E. Kuhn,²⁹ L. Lanza,¹⁶ M. Leali,^{39,19} S. Lee,²³ P. Lenisa,^{13,9} K. Livingston,⁴¹ I. J. D. MacGregor,⁴¹ D. Marchand,²⁰ L. Marsicano,¹⁵ V. Mascagna,^{38,19,§} B. McKinnon,⁴¹ C. McLauchlin,³⁴ S. Migliorati,^{39,19} M. Mirazita,¹⁴ V. Mokeev,³⁶ R. A. Montgomery,⁴¹ C. Munoz Camacho,²⁰ P. Nadel-Turonski,³⁶ P. Naidoo,⁴¹ K. Neupane,³⁴ T. R. O'Connell,⁵ M. Osipenko,¹⁵ M. Ouillon,²⁰ P. Pandey,²⁹ M. Paolone,^{27,35} L. L. Pappalardo,^{13,9} R. Paremuzyan,^{36,26} E. Pasyuk,³⁶ W. Phelps,^{4,12} O. Pogorelko,²⁵ J. Poudel,²⁹ J. W. Price,² Y. Prok,²⁹ B. A. Rau,¹⁰ T. Reed,¹⁰ M. Ripani,¹⁵ A. Rizzo,^{16,32} P. Rossi,³⁶ J. Rowley,²⁸ F. Sabatié,³ A. Schmidt,¹² E. P. Segarra,²³ Y. G. Sharabian,³⁶ E. V. Shirokov,³³ U. Shrestha,^{5,28} D. Sokhan,^{3,41} O. Soto,^{14,37} N. Sparveris,³⁵ I. I. Strakovsky,¹² S. Strauch,³⁴ N. Tyler,³⁴ R. Tyson,⁴¹ M. Ungaro,³⁶ S. Vallarino,¹³ L. Venturelli,^{39,19} H. Voskanyan,⁴⁵ A. Vossen,^{6,36} E. Voutier,²⁰ D. P. Watts,⁴² K. Wei,⁵ X. Wei,³⁶ R. Wishart,⁴¹ B. Yale,⁴⁴ N. Zachariou,⁴² J. Zhang,⁴³ and Z. W. Zhao⁶

(CLAS Collaboration)

→ P. Chatagnon et al. (CLAS), PRL 127, 262501 (2021)

Future of TCS

- ▶ Experiments at JLab
- ▶ Prospects for EIC
 - ▶ Yellow Report: *Confronting DVCS and TCS results together is a mandatory goal of the EIC to prove the consistency of the collinear QCD factorization framework and to test the universality of GPDs.*
 - ▶ Preliminary predictions see Daria Sokhan talk at DIS2022
 - ▶ TCS included in EPIC, event generator for exclusive processes, interfaced to PARTONS (e-Print: 2205.01762 [hep-ph]), see also Kemal Tezgin talk at DIS2022
- ▶ Ultraperipheral Collisions at the LHC

Coefficient functions and Compton Form Factors

CFFs are the GPD dependent quantities which enter the amplitudes. They are defined through relations:

$$\begin{aligned}\mathcal{A}^{\mu\nu}(\xi, t) = -e^2 \frac{1}{(P + P')^+} \bar{u}(P') & \left[g_T^{\mu\nu} \left(\mathcal{H}(\xi, t) \gamma^+ + \mathcal{E}(\xi, t) \frac{i\sigma^{+\rho} \Delta_\rho}{2M} \right) \right. \\ & \left. + i\epsilon_T^{\mu\nu} \left(\tilde{\mathcal{H}}(\xi, t) \gamma^+ \gamma_5 + \tilde{\mathcal{E}}(\xi, t) \frac{\Delta^+ \gamma_5}{2M} \right) \right] u(P),\end{aligned}$$

where:

$$\begin{aligned}\mathcal{H}(\xi, t) &= + \int_{-1}^1 dx \left(\sum_q T^q(x, \xi) H^q(x, \xi, t) + T^g(x, \xi) H^g(x, \xi, t) \right) \\ \tilde{\mathcal{H}}(\xi, t) &= - \int_{-1}^1 dx \left(\sum_q \tilde{T}^q(x, \xi) \tilde{H}^q(x, \xi, t) + \tilde{T}^g(x, \xi) \tilde{H}^g(x, \xi, t) \right).\end{aligned}$$

Spacelike vs Timelike

D.Mueller, B.Pire, L.Szymanowski, J.Wagner, Phys.Rev.D86, 2012.

Thanks to simple spacelike-to-timelike relations, we can express the timelike CFFs by the spacelike ones in the following way:

$${}^T \mathcal{H} \stackrel{\text{LO}}{=} {}^S \mathcal{H}^*,$$

$${}^T \tilde{\mathcal{H}} \stackrel{\text{LO}}{=} -{}^S \tilde{\mathcal{H}}^*,$$

$${}^T \mathcal{H} \stackrel{\text{NLO}}{=} {}^S \mathcal{H}^* - i\pi Q^2 \frac{\partial}{\partial Q^2} {}^S \mathcal{H}^*,$$

$${}^T \tilde{\mathcal{H}} \stackrel{\text{NLO}}{=} -{}^S \tilde{\mathcal{H}}^* + i\pi Q^2 \frac{\partial}{\partial Q^2} {}^S \tilde{\mathcal{H}}^*.$$

The corresponding relations exist for (anti-)symmetric CFFs \mathcal{E} ($\tilde{\mathcal{E}}$).

DVCS CFFs from Artificial Neural Network fit - PARTONS

H. Moutarde, P. Sznajder, J. Wagner, Eur.Phys.J. C79 (2019)

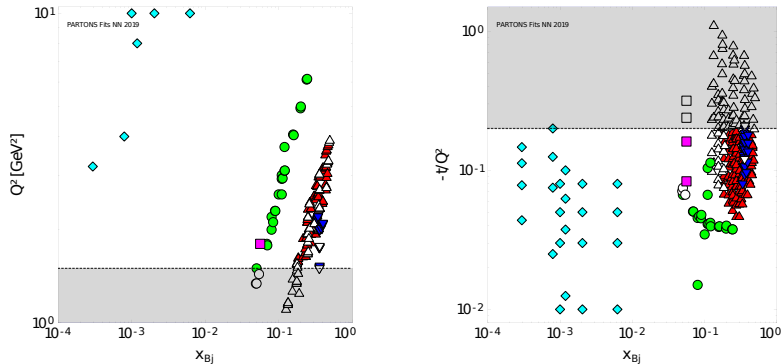


Figure: Coverage of the (x_{Bj}, Q^2) (left) and $(x_{Bj}, -t/Q^2)$ (right) phase-spaces by the experimental data used in DVCS CFFs fit. The data come from the Hall A (\blacktriangledown , \triangledown), CLAS (\blacktriangle , \triangle), HERMES (\bullet , \circ), COMPASS (\blacksquare , \square) and HERA H1 and ZEUS (\blacklozenge , \lozenge) experiments. The gray bands (open markers) indicate phase-space areas (experimental points) being excluded from this analysis due to the cuts.

DVCS vs TCS CFFs

O. Grocholski, H. Moutarde, B. Pire, P. Sznajder, J. Wagner, Eur.Phys.J. C80 (2020)

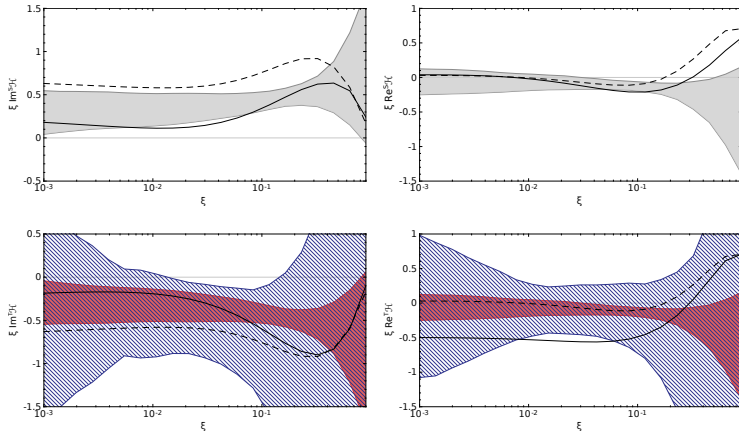


Figure: Imaginary (left) and real (right) part of DVCS (up) and TCS (down) CFF for $Q^2 = 2 \text{ GeV}^2$ and $t = -0.3 \text{ GeV}^2$ as a function of ξ . The shaded red (dashed blue) bands correspond to the data-driven predictions coming from the ANN global fit of DVCS data and they are evaluated using LO (NLO) spacelike-to-timelike relations. The dashed (solid) lines correspond to the GK GPD model evaluated with LO (NLO) coefficient functions.

TCS and Bethe-Heitler contribution to exclusive lepton pair photoproduction.

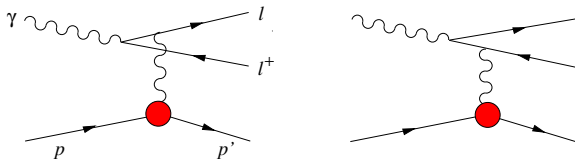


Figure: The Feynman diagrams for the **Bethe-Heitler** amplitude.

The cross-section for photoproduction of a lepton pair:

$$\frac{d\sigma}{dQ'^2 \ dt \ d\phi \ d\cos\theta} = \frac{d(\sigma_{\text{BH}} + \sigma_{\text{TCS}} + \sigma_{\text{INT}})}{dQ'^2 \ dt \ d\phi \ d\cos\theta}$$

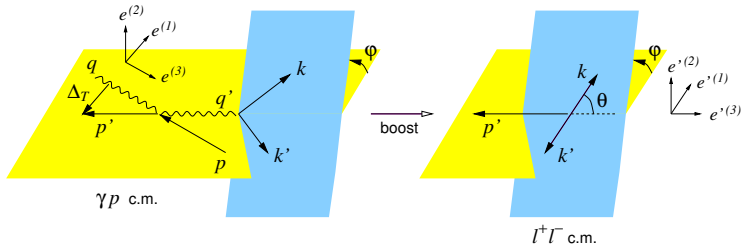


Figure: Kinematical variables and coordinate axes in the γp and $\ell^+ \ell^-$ c.m. frames.

$$\frac{d\sigma}{dQ'^2 dt d\phi d\cos\theta}$$

- ▶ Important to measure ϕ !
- ▶ BH dominates at θ close to 0 and π !

Interference

B-H dominant for not very high energies (JLAB), at higher energies the TCS/BH ratio is bigger due to growth of the gluon and sea densities.

Pire, Szymanowski, JW PRD 83

Moutarde, Pire, Sabatié, Szymanowski, JW PRD 87

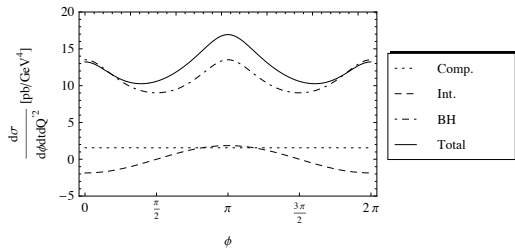


Figure: The differential cross section for $t = -0.2 \text{ GeV}^2$, $Q'^2 = 5 \text{ GeV}^2$, and integrated over $\theta \in (\pi/4, 3\pi/4)$ as a function of ϕ , for $s = 10^3 \text{ GeV}^2$.

Interference

- The **interference** part of the cross-section for $\gamma p \rightarrow \ell^+ \ell^- p$ with unpolarized protons and photons is given by:

$$\frac{d\sigma_{INT}}{dQ'^2 dt d\cos\theta d\varphi} \sim \cos\varphi \cdot \operatorname{Re} \mathcal{H}(\xi, t) \leftarrow \text{Sensitivity to the D-term!}$$

R ratio:

$$R = \frac{\frac{2}{dQ'^2} \int_0^{2\pi} \cos\phi \, d\phi \int_{\pi/4}^{3\pi/4} d\theta \frac{dS}{dQ'^2 dt d\phi d\theta}}{\int_0^{2\pi} d\phi \int_{\pi/4}^{3\pi/4} d\theta \frac{dS}{dQ'^2 dt d\phi d\theta}},$$

Forward Backward Asymmetry (from Pierre Chatagnon PhD thesis):

$$A_{FB}(\theta, \phi) = \frac{d\sigma(\theta, \phi) - d\sigma(180^\circ - \theta, 180^\circ + \phi)}{d\sigma(\theta, \phi) + d\sigma(180^\circ - \theta, 180^\circ + \phi)}$$

- The **interference** part depending on photons circular polarization ν :

$$\frac{d\sigma_{INT}}{dQ'^2 dt d\cos\theta d\varphi} \sim \nu \sin\varphi \cdot \operatorname{Im} \mathcal{H}(\xi, t)$$

Circular asymmetry

The photon beam **circular polarization** asymmetry:

$$A_{CU} = \frac{\sigma^+ - \sigma^-}{\sigma^+ + \sigma^-} \sim Im(H)$$

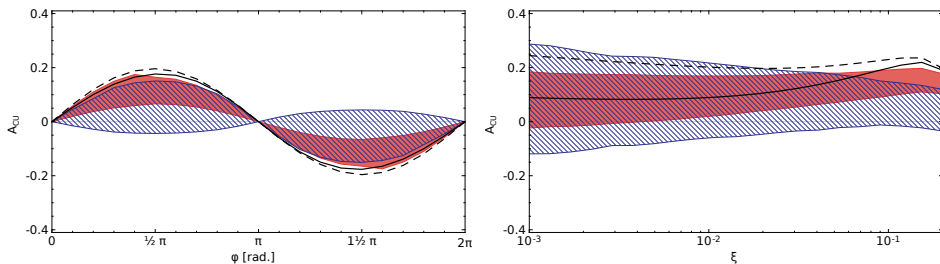


Figure: Circular asymmetry A_{CU} evaluated with LO and NLO spacelike-to-timelike relations for $Q'^2 = 4 \text{ GeV}^2$, $t = -0.1 \text{ GeV}^2$ and (left) $E_\gamma = 10 \text{ GeV}$ as a function of ϕ (right) and $\phi = \pi/2$ as a function of ξ . The cross sections used to evaluate the asymmetry are integrated over $\theta \in (\pi/4, 3\pi/4)$.

Transverse target asymmetry

$$\frac{d\sigma_{\text{INT}}^{\text{tpol}}}{dQ'^2 d(\cos \theta) d\phi dt d\varphi_S} \sim \sin \varphi_S \Im \left[\mathcal{H} - \frac{\xi^2}{1-\xi^2} \mathcal{E} + \tilde{\mathcal{H}} + \frac{t}{4M^2} \tilde{\mathcal{E}} \right].$$

The transverse spin asymmetry:

$$A_{UT}(\varphi_S) = \frac{\sigma(\varphi_S) - \sigma(\varphi_S - \pi)}{\sigma(\varphi_S) + \sigma(\varphi_S - \pi)},$$

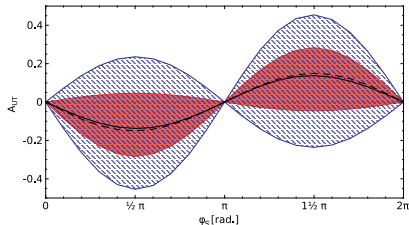
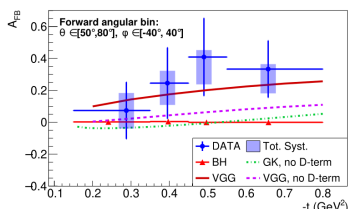
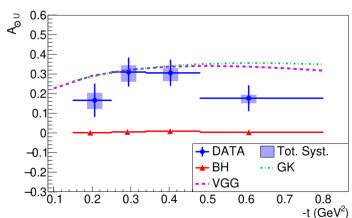
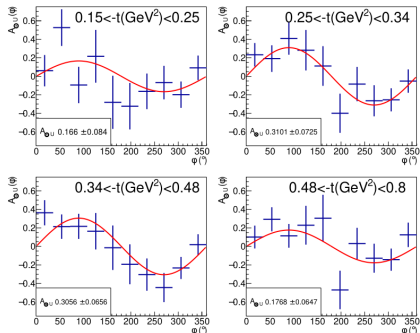


Figure: Transverse target spin asymmetry A_{UT} evaluated with LO and NLO spacelike-to-timelike relations for $Q'^2 = 4 \text{ GeV}^2$, $t = t_0$ and $E_\gamma = 10 \text{ GeV}$ as a function of φ_S . The cross sections used to evaluate the asymmetry are integrated over $\theta \in (\pi/4, 3\pi/4)$.

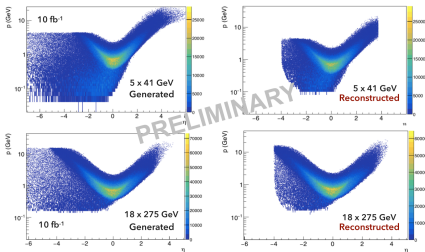
Results from CLAS12



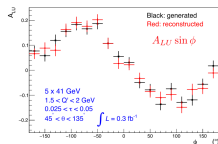
Preliminary prediction for EIC - D.Sokhan talk at DIS2022

Produced leptons: e^+e^-

Detected by the trackers and calorimeters in the central barrel.

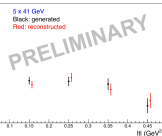


Beam-spin asymmetry



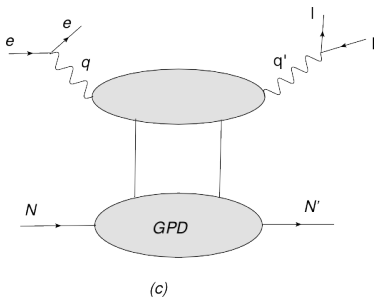
- Integrated luminosity: $\sim 0.3 \text{ fb}^{-1}$ (\sim two weeks of running).
- Agreement very good between generated and reconstructed asymmetries.

- Uncertainties are not purely statistical – fold in uncertainties on integrated cross-section from generator.
- Shape of t -distribution not important – artefact of generator before full optimisation.



Double DVCS

Belitsky & Muller, PRL 90, PRD 68, Guidal & Vanderhaeghen, PRL 90



(c)

$$\gamma^*(q_{in})N(p) \rightarrow \gamma^*(q_{out})N'(p')$$

$$\xi = -\frac{q_{out}^2 + q_{in}^2}{q_{out}^2 - q_{in}^2} \eta, \quad \eta = \frac{q_{out}^2 - q_{in}^2}{(p + p') \cdot (q_{in} + q_{out})}.$$

- ▶ DDVCS: $q_{in}^2 < 0, \quad q_{out}^2 > 0, \quad \eta \neq \xi$
- ▶ DVCS: $q_{in}^2 < 0, \quad q_{out}^2 = 0, \quad \eta = \xi > 0$
- ▶ TCS: $q_{in}^2 = 0, \quad q_{out}^2 > 0, \quad \eta = -\xi > 0$

Coefficient functions and Compton Form Factors

CFFs are the GPD dependent quantities which enter the amplitudes. They are defined through relations:

$$\begin{aligned}\mathcal{A}^{\mu\nu}(\xi, \eta, t) = -e^2 \frac{1}{(P + P')^+} \bar{u}(P') & \left[g_T^{\mu\nu} \left(\mathcal{H}(\xi, \eta, t) \gamma^+ + \mathcal{E}(\xi, \eta, t) \frac{i\sigma^{+\rho} \Delta_\rho}{2M} \right) \right. \\ & \left. + i\epsilon_T^{\mu\nu} \left(\tilde{\mathcal{H}}(\xi, \eta, t) \gamma^+ \gamma_5 + \tilde{\mathcal{E}}(\xi, \eta, t) \frac{\Delta^+ \gamma_5}{2M} \right) \right] u(P),\end{aligned}$$

,where:

$$\begin{aligned}\mathcal{H}(\xi, \eta, t) &= + \int_{-1}^1 dx \left(\sum_q T^q(x, \xi, \eta) H^q(x, \eta, t) + T^g(x, \xi, \eta) H^g(x, \eta, t) \right) \\ \tilde{\mathcal{H}}(\xi, \eta, t) &= - \int_{-1}^1 dx \left(\sum_q \tilde{T}^q(x, \xi, \eta) \tilde{H}^q(x, \eta, t) + \tilde{T}^g(x, \xi, \eta) \tilde{H}^g(x, \eta, t) \right).\end{aligned}$$

► DVCS vs TCS

$${}^{DVCS}T^q = -e_q^2 \frac{1}{x+\eta-i\varepsilon} - (x \rightarrow -x) = \left({}^{TCS}T^q\right)^*$$

$${}^{DVCS}\tilde{T}^q = -e_q^2 \frac{1}{x+\eta-i\varepsilon} + (x \rightarrow -x) = -\left({}^{TCS}\tilde{T}^q\right)^*$$

$${}^{DVCS}Re(\mathcal{H}) \sim P \int \frac{1}{x \pm \eta} H^q(x, \eta, t), \quad {}^{DVCS}Im(\mathcal{H}) \sim i\pi H^q(\pm\eta, \eta, t)$$

► DDVCS

$${}^{DDVCS}T^q = -e_q^2 \frac{1}{x+\xi-i\varepsilon} - (x \rightarrow -x)$$

$${}^{DDVCS}Re(\mathcal{H}) \sim P \int \frac{1}{x \pm \xi} H^q(x, \eta, t), \quad {}^{DVCS}Im(\mathcal{H}) \sim i\pi H^q(\pm\xi, \eta, t)$$

DDVCS can provide unique information, but is very challenging experimentally. But recent measurement of TCS should also make us more optimistic about DDVCS!

We need muon detection!

DDVCS - Calculation of amplitudes

New calculation using spinor techniques (Kleiss and Stirling):

$$i\mathcal{M}_{\text{DDVCS}}^{(V)} = -\frac{g_{\perp}^{\mu\nu}}{2}\bar{u}(\ell_-, s_\ell)\gamma_\mu v(\ell_+, s_\ell)\bar{u}(k', s)\gamma_\nu u(k, s)\mathcal{J}_{s_2 s_1}^+ ,$$

$$s(a, b) = \bar{u}(a, +)u(b, -) = -s(b, a) ,$$

$$t(a, b) = \bar{u}(a, -)u(b, +) = [s(b, a)]^* .$$

with:

$$s(a, b) = (a^2 + ia^3)\sqrt{\frac{b^0 - b^1}{a^0 - a^1}} - (a \leftrightarrow b) ,$$

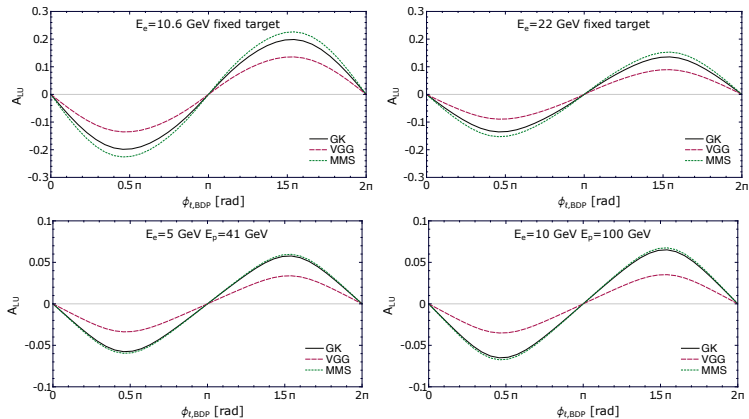
Final expressions in the form:

$$\begin{aligned} i\mathcal{M}_{\text{DDVCS}}^{(V)} = & -\frac{1}{2} \left[f(s_\ell, \ell_-, \ell_+; s, k', k) - g(s_\ell, \ell_-, n^*, \ell_+)g(s, k', n, k) - g(s_\ell, \ell_-, n, \ell_+)g(s, k', n^*, k) \right] \\ & \times \left[(\mathcal{H} + \mathcal{E})[Y_{s_2 s_1} g(+, r'_{s_2}, n, r_{s_1}) + Z_{s_2 s_1} g(-, r'_{-s_2}, n, r_{-s_1})] - \frac{\mathcal{E}}{M} \mathcal{J}_{s_2 s_1}^{(2)} \right] . \end{aligned}$$

where all $f, g, Y, Z, \mathcal{J}^{(2)}$ are given in terms of $s(a, b)$.

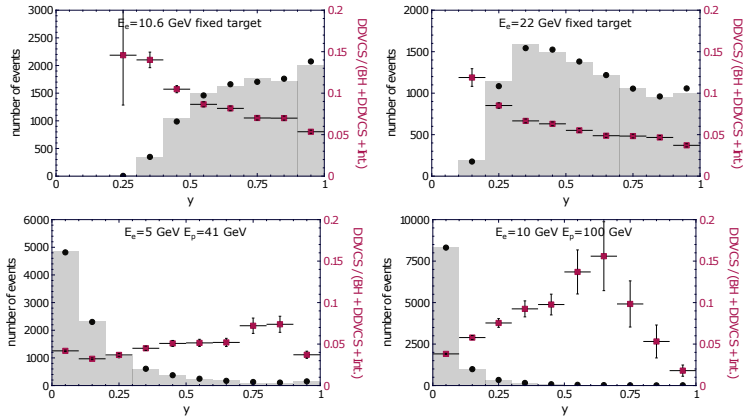
Results implemented in PARTONS and EPiC

Beam-Spin asymmetry in DDVCS



Experiment	Beam energies [GeV]	y	$ t $ [GeV 2]	Q^2 [GeV 2]	Q'^2 [GeV 2]
JLab12	$E_e = 10.6, E_p = M$	0.5	0.2	0.6	2.5
JLab20+	$E_e = 22, E_p = M$	0.3	0.2	0.6	2.5
EIC	$E_e = 5, E_p = 41$	0.15	0.1	0.6	2.5
EIC	$E_e = 10, E_p = 100$	0.15	0.1	0.6	2.5

DDVCS



Experiment	Beam energies [GeV]	Range of $ t $ [GeV 2]	$\sigma _{0 < y < 1}$ [pb]	$\mathcal{L}^{10\text{k}} _{0 < y < 1}$ [fb $^{-1}$]	y_{\min}	$\sigma _{y_{\min} < y < 1} / \sigma _{0 < y < 1}$
JLab12	$E_e = 10.6, E_p = M$	(0.1, 0.8)	0.14	70	0.1	1
JLab20+	$E_e = 22, E_p = M$	(0.1, 0.8)	0.46	22	0.1	1
EIC	$E_e = 5, E_p = 41$	(0.05, 1)	3.9	2.6	0.05	0.73
EIC	$E_e = 10, E_p = 100$	(0.05, 1)	4.7	2.1	0.05	0.32

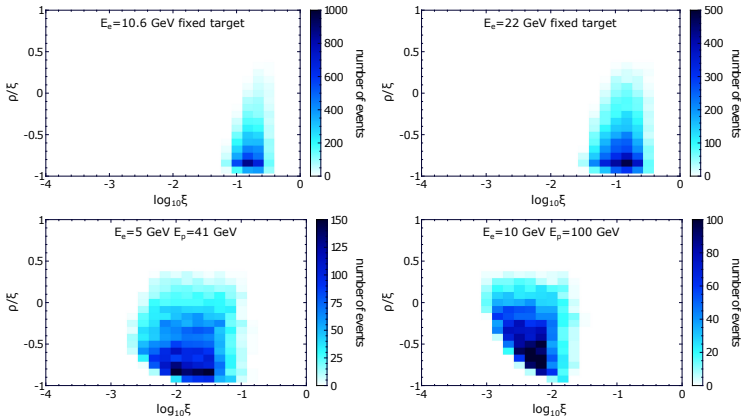
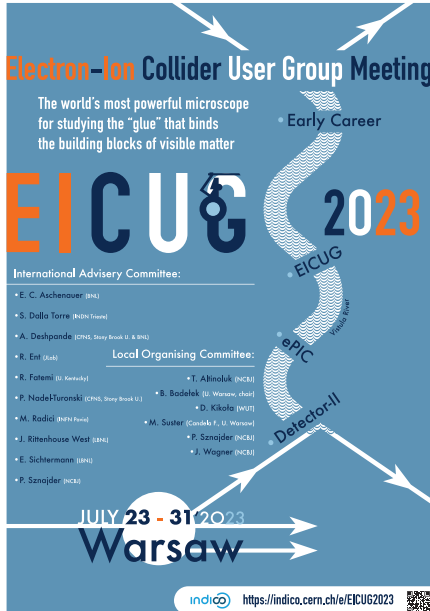


Figure: Distribution of Monte Carlo events as a function of the skewness variable ξ and the relative value of generalized Björken variable ρ . Each distribution is populated by 10000 events generated for the DDVCS sub-process at beam energies specified in the plot. Extra kinematical conditions, including cuts on the y variable, are specified in the paper.

Summary

- ▶ TCS is a mandatory complementary measurement to DVCS, cleanest way to test universality of GPDs. First measurement from CLAS12
- ▶ Timelike-spacelike relations at LO/NLO gives us tools to use TCS data in DVCS CFF fits, with special sensitivity to Q^2 dependence,
- ▶ First data-driven and model-free predictions for TCS using global DVCS data
- ▶ EIC - TCS study in Yellow Report, TCS included in EPiC event generator.
- ▶ Measurement of TCS should also make us more optimistic about the DDVCS, but **We need muon detection!**
- ▶ New analytical formulae for DDVCS have been derived.
- ▶ It is already implemented in PARTONS and EPiC MC generator (LO + LT).
- ▶ Asymmetries are large enough for DDVCS to be measurable at both current, JLab12, and future, JLab20+ and EIC, experiments.
- ▶ Addressing GPD model dependence with cross-sections and asymmetries is possible.



Early registration deadline: June 3th, 2023